Field-reversed configuration formed by in-vessel θ–pinch in a tandem mirror device

Munan Lin, Ming Liu, Guanghui Zhu, Peiyun Shi, Jian Zheng, Quanming Lu, and Xuan Sun

Citation: Review of Scientific Instruments **88**, 093505 (2017); doi: 10.1063/1.5001313
View online: http://dx.doi.org/10.1063/1.5001313
View Table of Contents: http://aip.scitation.org/toc/rsi/88/9
Published by the American Institute of Physics

Field-reversed configuration formed by in-vessel θ-pinch in a tandem mirror device

Munan Lin,[1,2] Ming Liu,[1,2] Guanghui Zhu,[1,2] Peiyun Shi,[1,2] Jian Zheng,[1,2] Quanming Lu,[2] and Xuan Sun[1,2,a)]
[1]*Department of Modern Physics, University of Science and Technology of China, Hefei 230026, China*
[2]*CAS Key Laboratory of Geospace Environment, No. 96, JinZhai Road Baohe District, 230026 Hefei, China*

(Received 27 February 2017; accepted 22 August 2017; published online 8 September 2017)

We describe a field reversed configuration (FRC) experiment featuring in-vessel θ-pinch coils and open-field-line plasmas confined in a tandem mirror. Two FRCs, formed near the west and the east mirror throats of a central cell, are ejected toward the mid-plane for colliding and merging. Each FRC consists of four groups of pulsed power supplies and four groups of coils, having diameters 35, 35, 40, and 45 cm. The rise time of the main reversal field is 7.15 μs, and the maximum voltage is 40 kV with total currents of 416 kA, corresponding to a magnetic field of 1690 G. The total capacitive stored energy is 115.2 kJ. A fast pulse gas injection system was designed and tested to inject neutral gas into the FRC formation region with controlled directions. The successful installation of the θ-pinch coils inside the vacuum vessel offers greater freedom for diagnostics and control instruments as well as preserving magnetic tandem mirror configuration. The magnetic field reversal is confirmed by internal magnetic field measurements. The plasma temperature, density, and lifetime are, respectively, ~100 eV, ~3.0×10^{18} m^{-3}, and ~300 μs for the current operating conditions. *Published by AIP Publishing.* [http://dx.doi.org/10.1063/1.5001313]

I. INTRODUCTION

The field reversed configuration (FRC) is a compact torus-shaped plasma confined predominantly by poloidal fields.[1–3] It possesses a closed-field-line plasma region that is enveloped by the separatrix, whereas outside open-field-line plasma are typically confined by mirror fields. The open-field-line region can also serve as a natural divertor for energy extraction and ash removal.[4,5] As a high β plasmoid ($\langle\beta\rangle = 2\mu_0\langle p\rangle/B_e^2 \sim 1$ is the ratio of average plasma pressure to the external confining magnetic pressure, where p is the plasma pressure and B_e is the external magnetic field), FRC has an edge over other fusion reactors for aneutronic fusion reaction such as D–He^3 and p–B^{11}. FRC can be formed by a variety of methods, such as θ-pinch,[1,3,6–10] translation-trapping,[11–17] collision-merging,[4,5,18–21] spheromak merging,[2,22] coaxial source,[2,23] and rotating magnetic fields.[24,25] Experiments in the past show that the FRC appears to be very robust as it can survive violent dynamics during the formation, translation, and merging,[5,16,18,20] making FRC research versatile.

We report in this paper the engineering efforts of a new colliding FRC experiment to be conducted in KMAX (Keda Mirror with AXisymmetricity) mirror machine. Compared with previous and existing FRC experiments, the KMAX-FRC has a distinctive feature: the in-vacuum θ-pinch coils. The compact toroidal plasmas, formed simultaneously by θ-pinch near the west and the east mirror throats of the central cell, are ejected toward the mid-plane for colliding and merging. The magnetic mirror ($B_M = 3600$ G, and the central cell's $B = 0$-500 G) is expected to play an important role in the confinement of the open-field-line plasma, which can lead to improvement of the FRC.

II. KMAX-FRC EXPERIMENTAL PLATFORM

A. KMAX machine description

The FRC θ-pinch coils are placed inside the main vessel of KMAX (Keda Mirror with AXisymmetricity), a tandem mirror, which consists of a central cell and two side cells. The axial length of the device without counting the plasma source or other parts attached to the endplate is 9.6 m and the central cell is 5.2 m. The inner diameters of the central chamber and the mirror throat are 1.2 m and 0.3 m, respectively, and the wall thickness is 10 mm. Three sets of turbo pumps, one 1200 l/s in each end cell and one 2000 l/s in the central cell, are used to pump the background pressure down to 6.0×10^{-7} Torr. For a typical magnetic field configuration (Fig. 1), the magnetic field at the mid-plane is 500 G. The maximum magnetic field at the mirror throat is 3600 G.

B. In-vacuum θ-pinch coils

A common practice is to have the θ-pinch coils outside the vacuum vessel, e.g., wrapping around a quartz tube.[8,10,16,26] However, as a non-conducting radial boundary, the quartz tube may affect the FRC's performance. A recent study from the C2 experiment shows that the edge plasma plays an important role in the stability of the FRC.[5,19] Unfortunately, the quartz tube, separating the FRC region from the endplate, can render less effective for many controls installed in the end cells. It also creates an unknown region because the volume surrounded by the tube is inaccessible for many diagnostics.

a)Author to whom correspondence should be addressed: xsun@ustc.edu.cn

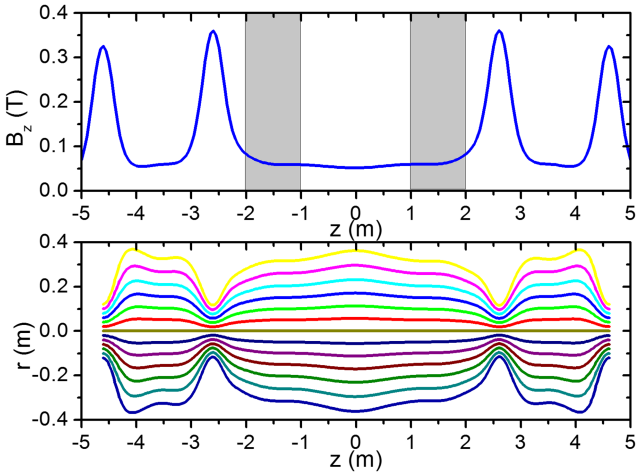

FIG. 1. Plots of axial magnetic field and magnetic flux. Grey shaded area indicates the positions of θ-pinch coils.

In this regard, one of the goals of KMAX-FRC is to explore the possibility of removing this quartz tube by placing the FRC coils inside the vacuum. Highlighted by color in Fig. 2, the four sets of theta-pinches are located on each side of the chamber. Each set has four loops in parallel, which is made of copper, 5.0 cm in width and 0.5 cm in thickness, and the distance between each loop is 1.5 cm. The west and the east FRC coils are symmetrically installed inside the central cell from $z = -2.0$ to -1.0 m and $z = 1.0$ to 2.0 m, respectively. The first two sets near the mirror throat are both 35 cm, and the third and fourth sets are, respectively, 40 cm and 45 cm in inner diameter. The half-angle calculated from the first to last loop is about 2.8°, similar to that for the FRX-L conical theta-pinch. Each set is powered by an independent pulsed power unit, thus, KMAX-FRC can operate using either FRX-L's or C2's formation techniques.

To prevent the plasma–antenna interaction, Faraday shielding is employed in various heating experiments. In our case, the gas is injected into the FRC formation region for ionizing, so unless gas flow can be carefully controlled, Faraday shielding cannot be used because neutral gas may diffuse to the periphery of coils resulting in unwanted ionization or arcing. To simplify the design and reduce the engineering cost, we installed a quartz tube in the vessel merely for shielding neutrals and plasmas. Note that the quartz tube is not a vacuum boundary in our case. Gas is injected into the quartz tube using two sets of injectors. Each set consists of four gas lines (see Sec. II E for details). The total length of the formation tube is 1.125 m. Two circular glass plates are mounted on both ends of the formation tube to reduce direct contacts between neutrals to the coils (Fig. 3).

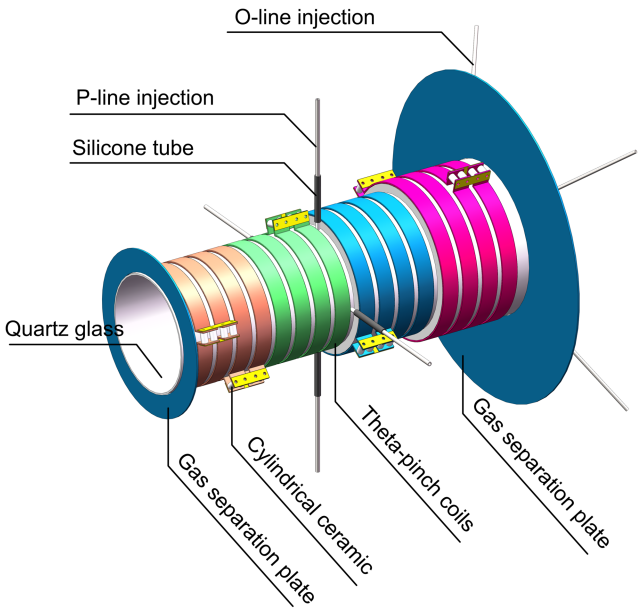

FIG. 3. Schematic of KMAX-FRC θ-pinch coils. The diameters of these four groups of coils are 35, 35, 40, and 45 cm. The total length of the formation tube is 1.125 m.

C. Pulsed power system

The engineering design and electrical circuit of KMAX-FRC pulsed power system are illustrated in Figs. 4 and 5, respectively. For each formation stage, there is a 5 μF main field, a 2 μF pre-ionization (PI), and a 50 μF bias field capacitor in series with a 55 μH air core inductor to power up the θ-pinch coils. Detailed parameters can be found in Table I. In Fig. 5, $H1 - H4$ represents high voltage switches; $L1$ represents a group of θ-pinch coils, ~0.3 μH; $L2$ represents a 55 μH air core inductor for a slow bias field; and $L3$ represents the circuit stray inductance ~0.4 μH. The arrangement of switches and capacitors is given in Fig. 5.

Because of space limitation in the lab, two stainless steel cabinets sheathed in a 1.2 mm thick copper plate were designed and installed to site those capacitors inside two levels. The thickness of the stainless steel is 3 mm, which suffices for biological shielding. The cabinet has a side door for cable routing. For each pulse power unit, two copper terminal blocks, one each for the forward and return currents, are connected to the two electrodes of the capacitor banks. The terminal blocks are also connected to the in-vessel coils via four high voltage

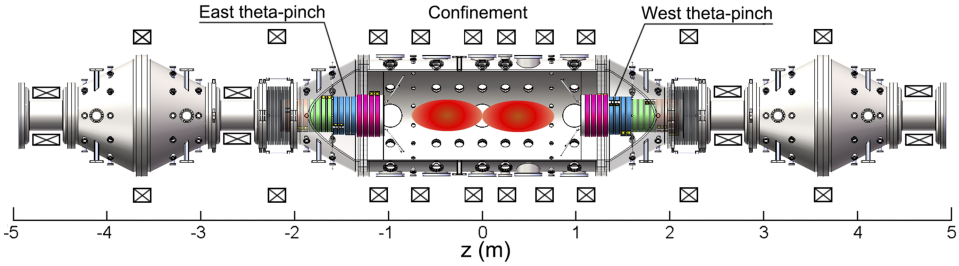

FIG. 2. Cutaway drawing of the KMAX-FRC. Its length is 9.6 m and the inner diameter of the central chamber is 1.2 m. Mirror coils are located at $z = -4.5$, -2.5, 2.5, and 4.5 m. Maximum mirror field is 3600 G. θ-pinch coils are from $z = -2.0$ to -1.0 m and $z = 1.0$ to 2.0 m.

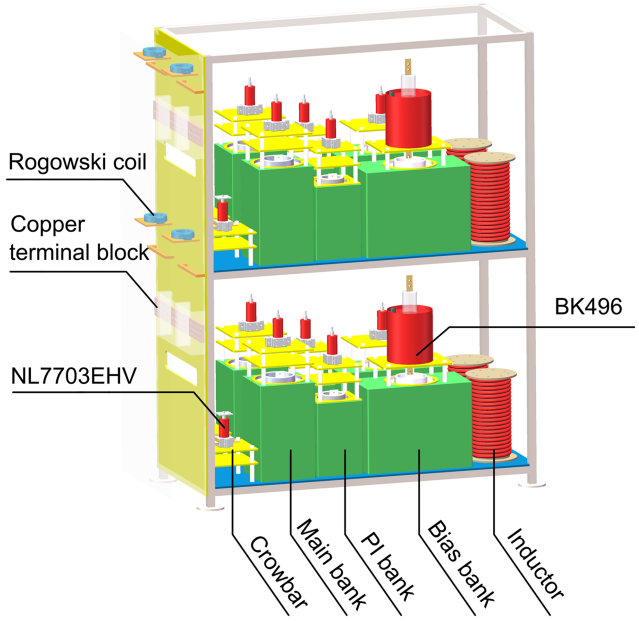

FIG. 4. Schematic of the KMAX-FRC pulsed power system. The main components are bias field bank modules, PI field modules, main field modules, ignition switches, 55 μH air core inductors, and Rogowski coils.

feed-through electrodes (see Fig. 6), again two each for the forward and return currents. The electrodes are connected to the θ-pinch coils via copper busbars inside the vacuum vessel. The cables used for the connection are 50 mm^2 silicone cables (Rating, 40 kV). The switches are mounted directly above the corresponding capacitors. The stainless-steel cabinet is grounded to an earthed electrode outside. None of the pulse power elements are directly connected to the KMAX chamber. The discharge currents of eight power units are measured by eight home-made Rogowski probes with 0.67 V/kA sensitivity and 200 kHz bandwidth.

D. Electrode feed-through inside vacuum

Perhaps one of the most challenging tasks of this experiment is to feed the high voltage high current into the vacuum chamber without arcing. We use a commercial vacuum break rated at voltage 40 kV, and a modified vacuum CF flange feed-through electrode by adding a 200 mm long ceramic tube (wall thickness, 10 mm) on the copper conductor (see Fig. 6), and the ceramic tube extends out by 3.5 cm to minimize arcing to the grounded chamber. The center conductor

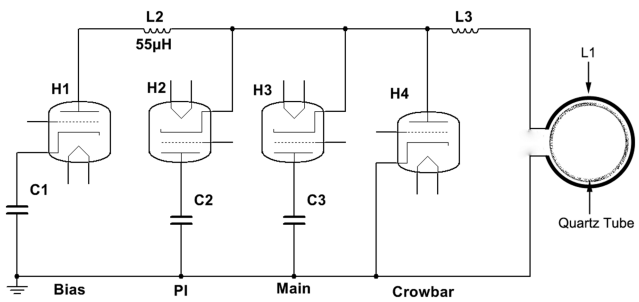

FIG. 5. Electrical circuit of the KMAX-FRC pulsed power system.

TABLE I. KMAX-FRC parameters.

Parameter	Unit	Bias banks	PI banks	Main banks
Bank voltage	kV	−20	20	40
Bank capacity	μF	50 × 8	2 × 8	5 × 8
Bank energy	kJ	80	3.2	32
Bank inductance	nH	≤300	≤50	≤50
Bank resistance	mΩ	≤100	≤50	≤50
Quarter-cycle	μs	81.25	3.70	7.15
Maximum current	kA	17 × 8	16 × 8	52 × 8
Maximum magnetic field	G	552	520	1690

is 20 mm in diameter, 230 mm in length, and a rectangular copper block, 60 mm × 20 mm × 30 mm ($L \times W \times H$), with through-holes of 9 mm diameter is welded to it for cable connection. For additional protection, a polytetrafluoroethylene (PTFE) plate (Fig. 6) is placed on the end of the conductor to further block the possible arcing path from the ground to the copper tip. As described above, there are four formation stages on each side, each stage comprising of four parallel copper coils. In the future, we may increase the formation stages to eight on each side, i.e., one stage corresponding to two parallel copper coils. Hence in the vacuum chamber two copper coils are connected to one electrode. In other words, for one power unit, there are currently two pairs of such feed-through electrodes for forward and return currents. Hence, in total, there are 32 feed-through electrodes, and all of them are mounted on 2-3/4-in. CF ports of the tapered vacuum chamber between the main vessel and the mirror throat. These electrodes have been tested for tens of kilovolts and tens of thousands amperes. Not shown in Fig. 6 is a 1.2-mm-thick copper Faraday cage enclosing all the electrodes and cables to shield the EM pulse.

E. Pulse gas injection system

The initial gas distribution has been considered a key to the formation of a high quality FRC. Any non-ionized gas may degrade the FRC's performance especially for neutrals that diffuse into the main vessel where the FRC colliding takes place. Two sets of gas-puffing injecting systems have been designed and installed. Each set consists of four gas puffing lines, distributed symmetrically on a plane. The P-lines

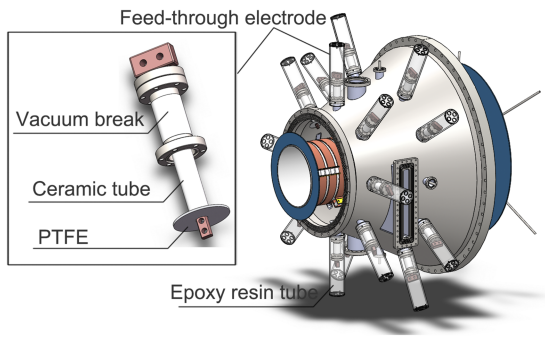

FIG. 6. Schematic of feed-through electrodes mounted on the tapered chamber. The inset figure shows a magnified view of an in-vacuum electrode feed-through.

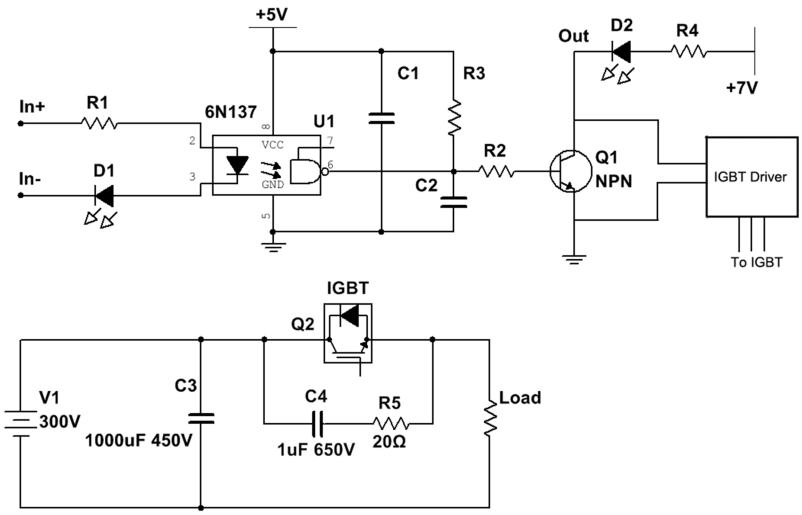

FIG. 7. Electrical circuit of the gas-valve driver.

(perpendicular injection) are right on the middle plane of the quartz tube and inject the gas perpendicularly. The O-lines (oblique injection) are installed on the main vessel near the exit of the quartz tube and inject the gas obliquely towards the center point of the quartz tube. Hence, the O-line injected gas flows towards the east/west ends so the neutrals in the central cell can be minimized. In total, there are 16 gas lines with 16 electromagnetic inlet valves. Among them, eight are P-line valves installed on eight 2-3/4-in. CF flanges on the tapered chambers and the other eight are O-line valves on eight 6-in. CF flanges on the central confinement chamber. All valves on KMAX are DJ2B inlet electromagnetic valves (SevenStar, Inc.). Instead of using the manufacturer's power supply, we developed our own pulse generator to open and close the valve in less than 4 ms. A schematic circuit of the gas-valve driver is shown in Fig. 7. A 450 V, 1000 μF electrolytic capacitor supplies the initial high voltage. It is charged with a 1000 V regulated DC power supply. A Transistor-Transistor Logic (TTL) trigger signal is sent from the control room to turn on the Insulated Gate Bipolar Transistor (IGBT) to energize the electromagnetic valve driver. To reduce the electrical surge caused by rapid falling off of current, a snubber circuit consisting of a 1 μF, 650 V capacitor and a 20 Ω non-inductive resistor in parallel with IGBT is developed for this circuit.

Figure 8 shows the temporal evolution of neutral pressure at two different locations measured using a fast ion gauge. The puff valve driver is triggered at $t = 0$, and the pressure at $z = 1.5$ m and $z = 4.5$ m starts to rise at $t = 4$ ms and $t = 7$ ms, respectively. Note that the data were taken with the same gauge by changing its location. The gas diffusion velocity calculated from the time difference is ~1 km/s.

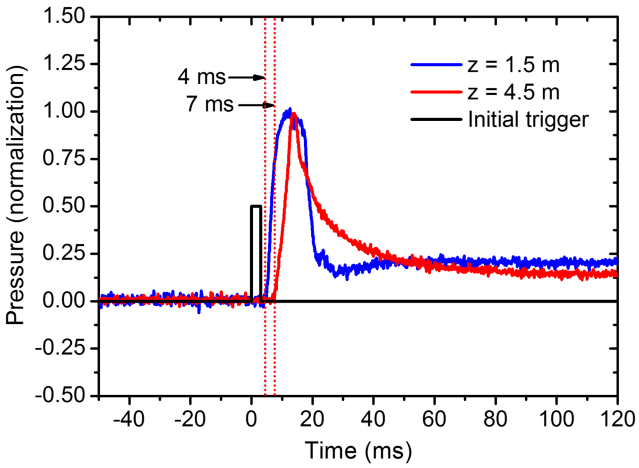

FIG. 8. Temporal evolution of neutral gas pressure measured by a fast ion gauge. The data were taken at $z = 1.5$ m (blue curve) and $z = 4.5$ m (red curve) for 0.2 MPa pressure.

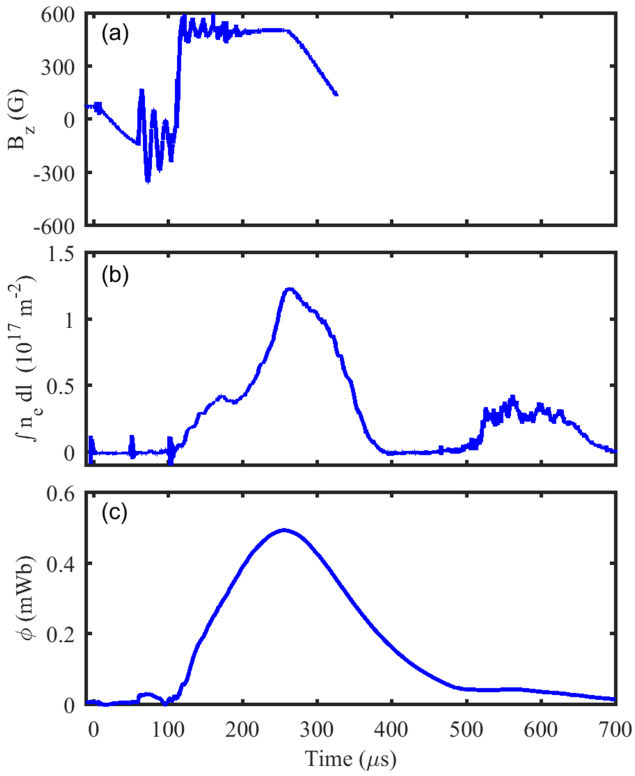

FIG. 9. (a) The magnetic waveform produced by θ-pinch current. (b) Line integrated density measured by a microwave interferometer at z = −0.25 m; the distance of the microwave chord to the axis is 12.6 cm. (c) Magnetic flux measured by a diamagnetic loop at $z = 0.33$ m. The background magnetic field strength in the central cell is 80 G.

III. INITIAL RESULTS

As stated above, the plasmas are created by pulsing θ-pinches simultaneously in the west and the east sides of the central cell, which are then ejected toward the mid-plane for colliding and merging. The switching sequence for generating FRC plasma is described as follows: (1) At $t = 4$ μs, a trigger signal is applied to the $H1$ switch to switch on a 50 μF capacitor bank and produce a bias magnetic field B_0 up to 227 G with a quarter periods of ~81.25 μs. (2) At $t = 59$ μs, the $H2$ switch is triggered. A 2 μF capacitor bank generates a 67.5 kHz oscillating electromagnetic field to ionize the argon gas, which produces a cold but sufficiently conducting plasma to freeze the bias magnetic field. (3) At $t = 111$ μs, after 2–3 PI oscillation periods, the third trigger signal is sent to the $H3$ switch to switch on the 5 μF capacitor bank to produce the main reversal field. Its rise time is 7.15 μs. (4) At $t = 117$ μs, to prevent the circuit's oscillation, the $H4$ switch, i.e., the crowbar switch, is turned on near the maximum of the main field. The crowbar switch allows the current in the circuit to decay over time L/R, reducing ringing in the circuit. The corresponding magnetic waveform is shown in Fig. 9(a), with capacitor banks of bias, pre-ionization, and main charged to −8, 10, and 17 kV, respectively.

Currently, we use argon as the working gas and the plasma can be reliably produced. Figure 9(b) shows the line-integrated plasma density measured by a microwave interferometer at $z = -0.25$ m with an impact parameter of 12.6 cm. Figure 9(c) shows the flux amplitude measured by a diamagnetic loop at $z = 0.33$ m, and Fig. 10 is the radial density profile measured by a triple probe at $z = -0.5$ m. Though the density profile is slightly different from the ideal profile that one would expect for a FRC, it may be due to the perturbation introduced by the probe.

Figure 11 is the internal field structure measured by a magnetic probe array at $z = -0.5$ m. Clearly the fields are reversed in the center. The data also indicate the separatrix radius $r_s \sim 18$ cm. Using the radial pressure balance model, the average $\langle\beta\rangle = 1 - \frac{r_s^2}{2r_w^2}$, where r_w is the radius of wall, one can thus estimate the total temperature of KMAX-FRC plasma, $T_e + T_i$, is ~100 eV.

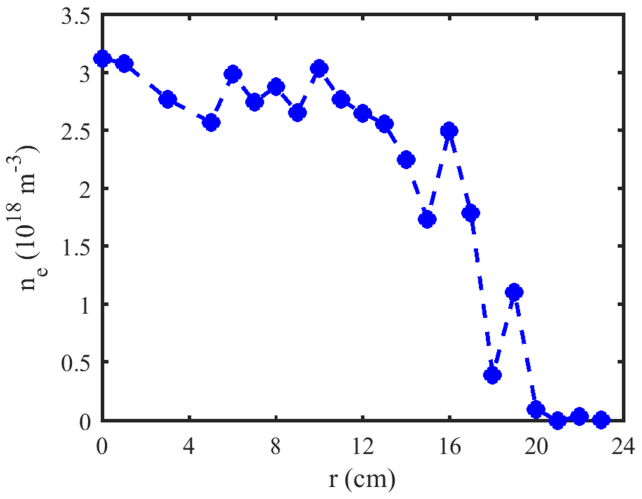

FIG. 10. Radial density profile measured by a triple probe. The background magnetic field strength in the central cell is 270 G.

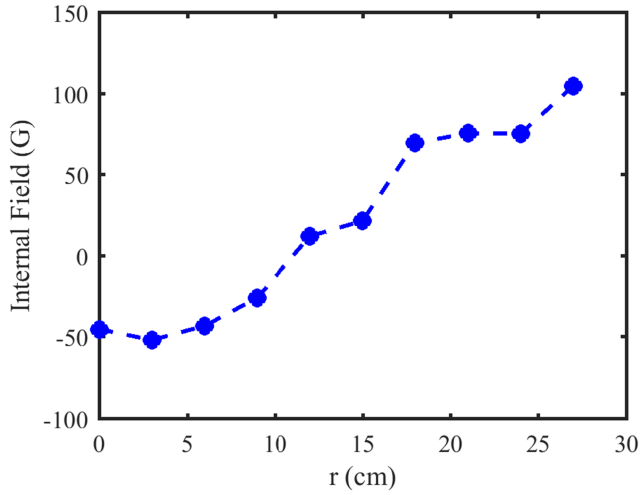

FIG. 11. Radial profile of internal magnetic field $B_z(r)$ at $t = 250$ μs, measured by a magnetic probe array. The background magnetic field strength in the central cell is 80 G.

IV. CONCLUSION

In summary, a FRC experiment has been set up on KMAX, and plasma has been achieved using a PI ringing technique. Many precautionary measures have been taken to prevent arcing with the installation of the θ-pinch coils inside the vacuum vessel. Nonetheless, the success of KMAX-FRC operation has proven its viability, paving the way to a possible better design, such as a dedicated rectangular port for current feed-through. These efforts have been rewarded with a machine that has flexibility in operation, as well as preserving the tandem-mirror magnetic field configuration, which may turn out to be a key component for future study. The formation of FRC is demonstrated by the magnetic probe measurements. The triple probe measurements indicate that the density is up to 3.0×10^{18} m^{-3}. The separatrix radius at z = −0.5 m is ~18 cm estimated from the internal magnetic probe measurement. The total temperature is ~100 eV derived from the radial pressure balance model, and the plasma lifetime is ~300 μs. In the future, the main research topics regarding the KMAX-FRC include the study of colliding and merging processes for the FRC, and how the magnetic mirror affects the FRC confinement by improving the open-field-line plasma parameters, as well as the engineering solution of forming a FRC without a quartz vacuum boundary.

ACKNOWLEDGMENTS

This work is supported by the National Natural Science Foundation of China (NSFC) under Grant No. 11475172, by the MOST of China under Grant No. 2013GB112007, and by the Chinese Academy of Sciences under Grant No. 2014.

[1]W. T. Armstrong, R. K. Linford, J. Lipson, D. A. Platts, and E. G. Sherwood, Phys. Fluids **24**, 2068 (1981).
[2]L. C. Steinhauer, Phys. Plasmas **18**, 070501 (2011).
[3]M. Tuszewski, Nucl. Fusion **28**, 2033 (1988).

[4]H. Y. Guo, M. W. Binderbauer, T. Tajima, R. D. Milroy, L. C. Steinhauer *et al.*, Nat. Commun. **6**, 6897 (2015).
[5]M. W. Binderbauer, T. Tajima, L. C. Steinhauer, E. Garate, M. Tuszewski *et al.*, Phys. Plasmas **22**, 056110 (2015).
[6]J. M. Taccetti, T. P. Intrator, G. A. Wurden, S. Y. Zhang, R. Aragonez *et al.*, Rev. Sci. Instrum. **74**, 4314 (2003).
[7]M. Tuszewski, W. T. Armstrong, R. E. Chrien, W. N. Hugrass, K. F. McKenna *et al.*, Phys. Fluids B **3**, 2844 (1991).
[8]T. Intrator, S. Y. Zhang, J. H. Degnan, I. Furno, C. Grabowski *et al.*, Phys. Plasmas **11**, 2580 (2004).
[9]T. P. Intrator, R. E. Siemon, and P. E. Sieck, Phys. Plasmas **15**, 042505 (2008).
[10]R. E. Siemon, W. T. Armstrong, D. C. Barnes, R. R. Bartsch, R. E. Chrien *et al.*, Fusion Technol. **9**, 13 (1986).
[11]H. Y. Guo, A. L. Hoffman, K. E. Miller, and L. C. Steinhauer, Phys. Rev. Lett. **92**, 245001 (2004).
[12]H. Y. Guo, A. L. Hoffman, R. D. Milroy, L. C. Steinhauer, R. D. Brooks *et al.*, Phys. Plasmas **15**, 056101 (2008).
[13]H. Y. Guo, A. L. Hoffman, L. C. Steinhauer, and K. E. Miller, Phys. Rev. Lett. **95**, 175001 (2005).
[14]H. Himura, S. Ueoka, M. Hase, R. Yoshida, S. Okada *et al.*, Phys. Plasmas **5**, 4262 (1998).
[15]A. L. Hoffman and J. T. Slough, Nucl. Fusion **33**, 27 (1993).
[16]S. Okada, T. Asai, F. Kodera, K. Kitano, Y. Suzuki *et al.*, Nucl. Fusion **41**, 625 (2001).
[17]S. Okada, K. Kitano, H. Matsumoto, K. Yamanaka, T. Ohtsuka *et al.*, Nucl. Fusion **39**, 2009 (1999).
[18]M. W. Binderbauer, H. Y. Guo, M. Tuszewski, S. Putvinski, L. Sevier *et al.*, Phys. Rev. Lett. **105**, 045003 (2010).
[19]H. Gota, M. Tuszewski, E. Trask, E. Garate, M. W. Binderbauer *et al.*, Fusion Sci. Technol. **68**, 44 (2015).
[20]H. Y. Guo, M. W. Binderbauer, D. Barnes, S. Putvinski, N. Rostoker *et al.*, Phys. Plasmas **18**, 056110 (2011).
[21]M. Tuszewski, A. Smirnov, M. C. Thompson, T. Akhmetov, A. Ivanov *et al.*, Phys. Plasmas **19**, 056108 (2012).
[22]S. P. Gerhardt, E. V. Belova, M. Yamada, H. Ji, Y. Ren *et al.*, Phys. Plasmas **15**, 032503 (2008).
[23]Y. Ono, M. Inomoto, Y. Ueda, T. Matsuyama, and T. Okazaki, Nucl. Fusion **39**, 2001 (1999).
[24]H. Y. Guo, A. L. Hoffman, R. D. Brooks, A. M. Peter, Z. A. Pietrzyk *et al.*, Phys. Plasmas **9**, 185 (2002).
[25]H. Y. Guo, A. L. Hoffman, and L. C. Steinhauer, Phys. Plasmas **12**, 062507 (2005).
[26]J. Slough, G. Votroubek, and C. Pihl, Nucl. Fusion **51**, 053008 (2011).